Supplementary Materials and Methods

Immunohistochemistry. Sections 4-5 microns thick prepared from formalin-fixed paraffin embedded tissues were dewaxed using Bond Dewax solution (Leica) and subjected to antigen retrieval using citrate antigen retrieval buffer, then primary antibody was applied. Immunoperoxidase staining was developed using the Leica Refine Detection kit followed by counterstaining with hematoxylin. Staining intensity was graded from I (no staining) to IV (strong staining), and GR staining of marrow stromal cells was used as an internal control to exclude false negative staining results. Photographs were taken on a Nikon Eclipse 80i microscope with a Nikon Digital Sight camera using NIS-Elements F2.30 software at a resolution of 2560 × 1920. Using Adobe Photoshop CS2, images were re-sized and set at a resolution of 300 pixels/inch. All images presented were obtained under identical optical conditions.

Targeted deep sequencing of *Nr3c1*. Leveraging ~400 ng of remaining libraries prepared for exome sequencing as described in the Materials and methods section, we pooled and captured by hybridization with baits specific to the coding exons of mouse *Nr3c1*. Capture pools were sequenced as described in the Materials and methods section to an average coverage of 10,000-fold with 100% of the targeted sequences having greater than 100-fold coverage. Development of this targeted deep sequencing assay was based on the analogous Mouse IMPACT (Integrated Mutation Profiling of Actionable Cancer Targets) (1). This assay captures all protein-coding exons and select introns of 578 cancer-associated genes mapped to the mouse genome, which are sequenced to an average of 637-fold coverage and cross-validated using exome sequencing of the same samples.

Exome and targeted sequencing analysis. All sequence data including read alignment; quality and performance metrics; post-processing, somatic mutation and DNA copy number alteration detection; and variant annotation were performed as previously described (2-4) using the mm10 build of the mouse genome. Briefly, reads were aligned with BWA (5), and processed using Picard tools and the Genome Analysis Toolkit (GATK) pipeline (6) followed by base quality recalibration and multiple sequence realignment. Somatic point mutations and indels were detected with MuTect (7) and Pindel (8) algorithms, respectively. Candidate mutations were manually reviewed using IGV (9). DNA copy number analysis was performed with ADTex (10) and loss of heterozygosity analysis was performed from germline heterozygous and homozygous SNPs called at a depth of 20x or greater in the treatment-naïve and resistant specimens with UnifiedGenotyper in GATK.

Sanger sequencing validation of *Nr3c1* mutations. Genomic DNA was extracted from bone marrow of recipient mice as described in the Materials and methods section, then subjected to PCR using *Taq* DNA Polymerase (New England BioLabs) with the primers listed in Table S6. Amplified DNA was purified using ExoSAP-IT PCR Product Cleanup Reagent (Thermo Fisher Scientific) and submitted for Sanger sequencing. Chromatograms were visualized using 4Peaks software. Peak signal strength for primary and minor peaks on chromatogram sequence traces were determined with the ThermoFisher Sanger Variant Analysis Tool. Peak ratios were calculated for the T-ALL 78A *Nr3c1* L282fs indel, averaged across the frameshifted region, and their allele fraction distribution was plotted using the box and whisker method (10-90th percentile).

RNA-seq analysis. Raw reads were assessed and processed to discard low quality reads, trim adaptor sequences, and eliminate poor quality bases with FastQC and Trimmomatic (11). Reads were aligned with Bowtie2 (12) mapping to the mm10 build of the mouse genome. Transcript quantification was performed with RNA-Seq Expectation Maximization (RSEM) (13). Quality control and normalization for read alignment and transcript quantification were performed using Picard tools and Exploratory Data Analysis (EDASeq) R package. Differential gene expression analysis was performed with edgeR (14) and gene set enrichment analysis (GSEA) was performed using the command-line version of the tool (15).

Supplementary References

1. Pronier E, Bowman RL, Ahn J, Glass J, Kandoth C, Merlinsky TR, et al. Genetic and epigenetic evolution as a contributor to WT1-mutant leukemogenesis. Blood. 2018 Sep 20;132(12):1265-78.

2. Iyer G, Hanrahan AJ, Milowsky MI, Al-Ahmadie H, Scott SN, Janakiraman M, et al. Genome sequencing identifies a basis for everolimus sensitivity. Science. 2012 Oct 12;338(6104):221.

3. Al-Ahmadie H, Iyer G, Hohl M, Asthana S, Inagaki A, Schultz N, et al. Synthetic lethality in ATM-deficient RAD50-mutant tumors underlies outlier response to cancer therapy. Cancer discovery. 2014 Sep;4(9):1014-21.

4. Burgess MR, Hwang E, Mroue R, Bielski CM, Wandler AM, Huang BJ, et al. KRAS Allelic Imbalance Enhances Fitness and Modulates MAP Kinase Dependence in Cancer. Cell. 2017 Feb 23;168(5):817-29 e15.

5. Li H, Durbin R. Fast and accurate short read alignment with Burrows-Wheeler transform. Bioinformatics. 2009 Jul 15;25(14):1754-60.

6. DePristo MA, Banks E, Poplin R, Garimella KV, Maguire JR, Hartl C, et al. A framework for variation discovery and genotyping using next-generation DNA sequencing data. Nature genetics. 2011 May;43(5):491-8.

7. Cibulskis K, Lawrence MS, Carter SL, Sivachenko A, Jaffe D, Sougnez C, et al. Sensitive detection of somatic point mutations in impure and heterogeneous cancer samples. Nature biotechnology. 2013 Mar;31(3):213-9.

8. Ye K, Schulz MH, Long Q, Apweiler R, Ning Z. Pindel: a pattern growth approach to detect break points of large deletions and medium sized insertions from paired-end short reads. Bioinformatics. 2009 Nov 1;25(21):2865-71.

9. Robinson JT, Thorvaldsdottir H, Winckler W, Guttman M, Lander ES, Getz G, et al. Integrative genomics viewer. Nature biotechnology. 2011 Jan;29(1):24-6.

10. Amarasinghe KC, Li J, Hunter SM, Ryland GL, Cowin PA, Campbell IG, et al. Inferring copy number and genotype in tumour exome data. BMC genomics. 2014 Aug 28;15:732.

11. Bolger AM, Lohse M, Usadel B. Trimmomatic: a flexible trimmer for Illumina sequence data. Bioinformatics. 2014 Aug 1;30(15):2114-20.

12. Langmead B, Salzberg SL. Fast gapped-read alignment with Bowtie 2. Nature methods. 2012 Mar 4;9(4):357-9.

13. Li B, Dewey CN. RSEM: accurate transcript quantification from RNA-Seq data with or without a reference genome. BMC bioinformatics. 2011 Aug 4;12:323.

14. Robinson MD, McCarthy DJ, Smyth GK. edgeR: a Bioconductor package for differential expression analysis of digital gene expression data. Bioinformatics. 2010 Jan 1;26(1):139-40.

15. Subramanian A, Tamayo P, Mootha VK, Mukherjee S, Ebert BL, Gillette MA, et al. Gene set enrichment analysis: a knowledge-based approach for interpreting genome-wide expression profiles. Proceedings of the National Academy of Sciences of the United States of America. 2005 Oct 25;102(43):15545-50.

Supplementary Tables

T-ALL	*Kras*	*Notch1*	median survival (days)			clonal evolution
			vehicle	DEX	DEX/GDC-0941	
5C	WT	WT	13	26	36	yes
4368	WT	WT	25.5	26	31	yes
8633	WT	mut	21.5	50	52	yes
JW-14	WT	WT	11	14	26	no
JW-81	WT	mut	20.5	42	58.5	no
2M	mut	mut	26.5	108	77	yes
20M	mut	mut	17.5	33	50	yes
73A	mut	mut	23.5	45	49	no
73M	mut	mut	11	26	28	no
78A	mut	mut	23.5	30	29	no

Table S1. RIM-induced T-ALLs show variable responses to DEX and DEX/GDC-0941 independent of *Kras* mutation status. Summary of survival data and mutation status for the 10 primary mouse T-ALLs represented in Figure 1b. Clonal evolution was defined as the emergence of one or more novel retroviral integrations on a Southern blot.

Brigham and Women's Hospital Cases					
Sample Number	**Site**	**Diagnostic Specimen**	**Relapse Specimen**	**Degree of Involvement (from core biopsy report)**	**Aspirate Count (percent blasts)**
1	BM	X		>90% blasts	Not available
2	BM	X		99% blasts	Not available
3	BM	X		95% blasts	Not available
4	BM	X		90% blasts	95%
5	BM	X		>90% blasts	65%
6	BM	X		>90% blasts	86%
7	BM	X		95% blasts	84%
8	BM	X		90% blasts	80%
9	BM	X		95% blasts	9%, *focally higher
10	BM	X		60-70% blasts	63%
11	BM	X		95% blasts	88%
12	BM	X		>90% blasts	72%
13	BM	X		5-10% blasts	9%
14	BM	X		>90% blasts	79%
15	BM	X		>95% blasts	89%
16	BM	X		80% blasts	89%
17	BM	X		>95% blasts	95%
18	BM	X		40-50% blasts	13%
19	BM	X		90% blasts	Not available
20	BM	X		>90% blasts	Not available
21	BM	X		70-75% blasts	Not available
22	BM	X		95% blasts	Not available
23	BM		X	>95% blasts	Not available
24	BM		X	90% blasts	91%
25	BM		X	40% blasts	40%
26	BM		X	>90% blasts	90%
27	BM		X	20-30% blasts	23%
28	BM		X	90% blasts	Not available
29	BM		X	>80% blasts	85%
30	BM		X	70-80% blasts	64%
31	BM		X	90% blasts	58%
32	BM		X	80% blasts	53%
33	BM		X	>90%	Not available
34	BM		X	90% blasts	Not available
35	BM		X	50% blasts	Not available
36	BM		X	90% blasts	Not available
37	KI		X	Diffuse	Not applicable
38	LN	X		Extensive	Not applicable
39	LN	X		Not indicated	Not applicable
40	LN		X	Diffuse	Not applicable
41	LN		X	Diffuse	Not applicable
42	MED	X		Diffuse	Not applicable
43	MED	X		Diffuse	Not applicable
44	SK	X		Diffuse	Not applicable
45	ST	X		Diffuse	Not applicable
46	ST		X	Diffuse	Not applicable
47	TE		X	Sheets	Not applicable

Boston Children's Hospital Cases			
Sample Number	**Diagnostic Specimen**	**Relapse Specimen**	**Aspirate Count (percent blasts)**
1	X		Not available
2	X		Not available
3	X		Not available
4	X		Not available
5	X		66%
6	X		72%
7	X		25%
8	X		52%
9	X		Not available
10	X		93%
11	X		Not available
12	X		Not available
13	X		11%
14	X		Not available
15	X		>95%
16	X		18%
17	X		2%
18	X		Not available
19	X		84%
20	X		95%
21	X		97%
22	X		70%
23	X		>95%
24	X		90%
25	X		>95%
26	X		>95%
27	X		93%
28	X		Not available
29	X		93%
30	X		>90%
31	X		75%
32	X		>95%
33	X		76%
34	X		83%
35	X		82%
36	X		69%
37	X		37%
38	X		58%
39	X		5%
40	X		80%
41	X		>95%
42	X		>95%
43		X	>90%
44		X	59%
45		X	88%

Table S2. Primary and relapsed human T-ALLs exhibit comparable leukemic blast percentages. For bone marrow core biopsies, histologic estimates of tumor involvement are reported as percentage of total bone marrow cells corresponding to leukemic blasts; qualitative descriptors of tumor involvement are provided for all other tissues (abstracted from original pathology reports). Formal blast counts derived from bone marrow aspirate samples are also provided for comparison. Classification as a diagnostic or relapsed specimen is indicated for each case. For Brigham and Women's Hospital cases, the specimen site is noted as follows: BM = bone marrow, KI = kidney, LN = lymph node, MED = mediastinum, SK = skin, ST = soft tissue, TE = testicle.

20M Relapse Specific Variants

Chr	Position	Ref	Alt	Gene Name	Amino Acid	Type	GO: glucocorticoid receptor signaling pathway	GO: negative/positive regulation of apoptotic process	20M.P VAF	20M.D1 VAF	20M.D2 VAF	20M.D4 VAF	20M.C1 VAF	20M.C3 VAF	20M.C5 VAF
1	127823423	A	C	Map3k19	p.N526K	missense			0	0	0	0.166	0.404	0.067	0.06
2	89617679	A	G	Olfr1248	p.V171A	missense			0	0	0	0	0	0.201	0
2	111449833	A	G	Olfr1287	p.D231G	missense			0	0.388	0	0	0	0	0
3	86291490	G	A	Erba	p.A205T	missense			0	0.467	0	0	0	0	0
3	114152655	G	A	Col11a1	p.G986D	missense			0	0	0	0	0.548	0	0
4	117229902	C	T	Gm1661	p.G189S	missense			0	0	0	0.222	0.403	0.125	0.058
4	141477012	C	A	Spen	p.D1435Y	missense			0	0	0	0.164	0.375	0.121	0.043
6	23410818	C	T	Cadps2	p.E705K	missense			0	0	0	0	0	0.278	0
7	127393324	C	T	E430018J23Rik	p.C38Y	missense			0	0	0	0.145	0.464	0	0
8	106255287	A	G	Smpd3	p.M647T	missense			0	0	0	0.184	0.455	0.047	0
8	109996825	G	A	Tat	p.R315Q	missense			0	0	0	0.29	0	0	0
9	38403203	T	C	Olfr147	p.S140P	missense			0	0	0	0	0.437	0	0
10	62864857	G	T	Tet1	p.T623K	missense			0	0	0	0	0	0.353	0
12	31074707	C	T	Fam110c	p.P223S	missense			0	0	0.383	0	0	0	0
13	119440813	T	C	Paip1	p.S114P	missense			0	0	0	0.175	0.488	0	0
14	118153661	G	A	Gpr180	p.G201R	missense			0	0	0.047	0.214	0.621	0.093	0.106
15	6773915	G	A	Rictor	p.A503T	missense			0	0	0	0	0	0.261	0
15	97748663	G	A	Rapgef3	p.S780F	missense			0	0	0.306	0	0	0	0
16	85868613	C	T	Adamts5	p.R600Q	missense			0	0	0	0	0.476	0	0
17	23291562	GC	G	Vmn2r114	p.A648fs	frameshift deletion			0	0	0	0	0.338	0	0
17	32701878	AACAGC	A	Cyp4f15	p.C377fs	frameshift deletion			0	0.316	0	0	0	0	0
17	33242719	G	C	Zfp955a	p.I146M	missense			0	0.241	0.216	0.186	0.179	0	0.245
17	34802359	C	T	Cyp21a1	p.R346H	missense			0	0.107	0.208	0.118	0.168	0.086	0.131
18	39422740	T	A	Nr3c1	p.K514X	stopgain	x	x	0	0.679	0	0	0	0	0
18	77441630	C	T	Loxhd1	p.R1990C	missense			0	0	0	0	0	0.241	0
19	5568962	T	G	Ap5b1	p.F137V	missense			0	0	0	0.175	0.398	0	0
X	17558787	A	G	Fundc1	p.V95A	missense			0	0	0	0	0.417	0	0

78A Relapse Specific Variants

Chr	Position	Ref	Alt	Gene Name	Amino Acid	Type	GO: glucocorticoid receptor signaling pathway	GO: negative/positive regulation of apoptotic process	78A.P VAF	78A.D1 VAF	78A.D4 VAF	78A.C2 VAF	78A.C3 VAF
3	145092204	C	A	Clca2	p.A167S	missense			0	0	0.354	0	0
4	128260424	T	C	Hmgb4	p.D117G	missense			0	0.299	0.062	0.333	0.412
7	96956049	AGTAG	A	Nars2	p.S83fs	frameshift deletion			0	0	0.352	0	0
7	103740830	T	C	Olfr629	p.T137A	missense			0	0.242	0.219	0.191	0.25
10	85120135	C	T	Mterf2	p.W208X	stopgain			0	0.412	0.385	0.398	0.445
11	115791861	G	A	2310067B10Rik	p.D575N	missense			0	0	0.354	0	0
13	34746963	G	A	Fam50b	p.E141K	missense			0	0.375	0	0.405	0.471
17	40207568	A	G	Pgk2	p.I323T	missense			0	0.104	0.345	0.108	0
18	39486387	T	TG	Nr3c1	p.L282fs	frameshift insertion	x	x	0.01	0.714	0.768	0.607	0.792
18	59048863	C	T	Adamts19	p.H1125Y	missense			0	0.212	0.057	0.075	0
19	11699517	G	A	Oosp3	p.G80E	missense			0	0.39	0.414	0.291	0.449

5C Relapse Specific Variants

Chr	Position	Ref	Alt	Gene Name	Amino Acid	Type	GO: glucocorticoid receptor signaling pathway	GO: negative/positive regulation of apoptotic process	5C.P VAF	5C.C3 VAF
3	7577208	T	C	Il7	p.N64S	missense		x	0	0.251
5	21646171	T	A	Armc10	p.C23X	stopgain		x	0	0.208
5	137525010	G	A	Gigyf1	p.G895S	missense			0	0.470
7	85737877	A	C	Vmn2r72	p.F826L	missense			0	0.264
7	87438089	C	T	Tyr	p.R405H	missense			0	0.238
10	129776574	T	C	Olfr809	p.L235P	missense			0	0.265
11	98328209	G	A	Neurod2	p.A43V	missense			0	0.200
18	39422731	G	A	Nr3c1	p.Q517X	stopgain	x	x	0	0.259
X	87304920	G	C	Il1rapl1	p.I131M	missense			0	0.135

2M Relapse Specific Variants

Chr	Position	Ref	Alt	Gene Name	Amino Acid	Type	GO: glucocorticoid receptor signaling pathway	GO: negative/positive regulation of apoptotic process	2M.P VAF	2M.C2 VAF
5	84106003	C	A	Epha5	p.L533F	missense			0	0.365
6	56986281	AC	A	Vmn1r5	p.T314fs	frameshift deletion			0	0.948
6	126642030	G	T	Kcna1	p.S442R	missense			0	0.535
10	88503821	AGCGCGGCG CCGGCCTGG CCCG	A	Chpt1	p.A5fs	frameshift deletion			0	0.300
17	32701878	AACAGC	A	Cyp4f15	p.C377fs	frameshift deletion			0	0.332
18	39422742	A	AT	Nr3c1	p.I513fs	frameshift insertion	x	x	0	0.553

Table S3. Relapse-specific variants and in parental and relapsed T-ALLs 20M, 78A, 5C and 2M. Summary of the variants identified by exome sequencing in relapsed T-ALLs shown in Figures 3 and 4 including information about GO terms related to glucocorticoid signaling and regulation of apoptosis, and variant allele frequency (with a threshold of 20%) in each parental and corresponding relapsed sample. Chr = chromosome, Ref = reference sequence, Alt = variant sequence, VAF = variant allele frequency.

Antibody	Clone
Glucocorticoid Receptor	D6H2L
Cleaved Notch1 (Val1744)	D3B8

PTEN	9552
Phospho-Akt (Ser473)	D9E
Akt (pan)	40D4
Phospho-p44/42 MAPK	D13.14.4E
p44/42 MAPK (Erk1/2)	3A7
Phospho-S6 Ribosomal	2F9
S6 Ribosomal Protein	54D2
GAPDH	D4C6R
Hsp90	68

Table S4. Primary antibodies used for Western blotting and immunohistochemistry. All antibodies listed were purchased from Cell Signaling Technology with the exception of Hsp90, which was purchased from BD Biosciences.

sgRNAs	**Sequence**
scramble	GGTTCTTGACTACCGTAATT
GR.guide.1	GGAATTCAGCAGGCCACTAC
GR.guide.2	TTCTTGTGAGACTCCTGTAG
HDR Template (listed 5' to 3')	TGTTTAAATACCCACAGCTCGAAAAACAAAGAAAA AAATATAAGGAATTCAGCAGGCCACCACAGGAGT CTCACAAGAAACCTCTGAAAATCCTGGTAACA
Primers	**Sequence**
forward	5'-ACCTCCAAGTCCAACGAGAGAGCC-3'
reverse	5'-ATGCCGTGGCTCATCCTTCATGC-3'
sequencing	5'-CCATGTCACTTTATCATAATTG-3'

Table S5. CRISPR/Cas9 reagents used for *Nr3c1* gene editing. Guides were designed to target the homologous region within exon 4 in which the *Nr3c1* mutation was identified in murine T-ALL 20M.D1. The HDR template was designed to incorporate the homologous base change identified in murine T-ALL 20M.D1, and was present in one of the two edited alleles of the GR3 CCRF-CEM cell clone shown in Figure 4.

78A Primers	**Sequence**
forward	5'-ACCTCCAAGTCCAACGAGAGAGCC-3'
reverse	5'-ATGCCGTGGCTCATCCTTCATGC-3

20M Primers	Sequence
forward	5'-GTACTCACGCCATGAACAGAAATG-3'
reverse	5'-AACAGCAAAATAGAAAAAGCCAGC-3'

Table S6. Primers used to amplify regions harboring *Nr3c1* mutations in murine T-ALLs. Primers were designed to amplify the regions within exon 1 of murine T-ALL 78A or exon 4 of murine T-ALL 20M in which *Nr3c1* mutations were identified by exome sequencing.

Gene	Assay Number
Gapdh	Mm99999915_g1
Nr3c1	Mm00433832_m1
Bcl2l11	Mm00437796_m1
Myc	Mm00487804_m1
Fkbp5	Mm00487406_m1
Tsc22d3	Mm00726417_s1

Table S7. Taqman Gene Expression Assays used for quantitative RT-PCR. Assays providing the best coverage were selected, and Taqman Gene Expression Master Mix also purchased from Applied Biosystems (product number: 4369016) was used.

Supplementary Figures

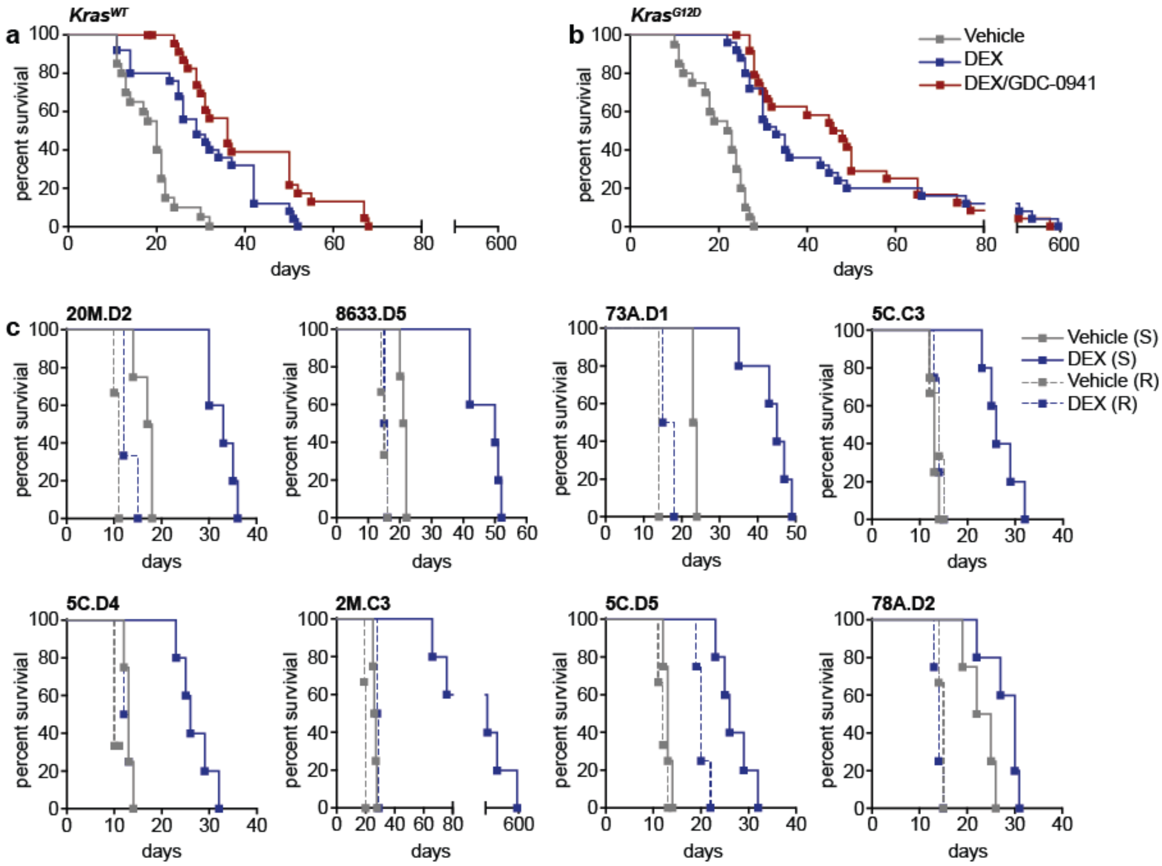

Figure S1. *Kras*^{WT} and *Kras*^{G12D} T-ALLs respond to DEX and the DEX/GDC-0941 combination and exhibit sustained resistance upon re-treatment. Kaplan-Meier survival analysis shows response to DEX or DEX/GDC-0941 in five *Kras*^{WT} (p-value<0.0001 for Vehicle vs. DEX, p-value=0.0218 for DEX vs. DEX/GDC-0941; Log-rank test) (**a**) and five *Kras*^{G12D} (p-value<0.0001 for Vehicle vs. DEX, p-value=0.5313 for DEX vs. DEX/GDC-0941; Log-rank test) (**b**) T-ALLs. **c** For each independent T-ALL, bone marrow isolated at relapse was re-transplanted into a new cohort of recipient mice and re-treated with DEX. Kaplan-Meier survival analysis shows response of resistant (R, dotted lines) T-ALLs treated with vehicle (n=3) or DEX (n=4) compared to the corresponding parental sensitive (S, solid lines) T-ALLs treated with vehicle (n=4) or DEX (n=5). Resistant T-ALLs demonstrated significantly shorter survival after DEX treatment versus the corresponding parental leukemias; 20M.D2 (p=0.0046, Log-rank test), 8633.D5 (p=0.0039, Log-rank test), 73A.D1 (p=0.0082, Log-rank test), 5C.C3 (0.0029, Log-rank test), 5C.D4 (p=0.0221, Log-rank test), 2M.C3 (p=0.0082, Log-rank test), 5C.D5 (p=0.0029, Log-rank test), 78A.D2 (p=0.0029, Log-rank test).

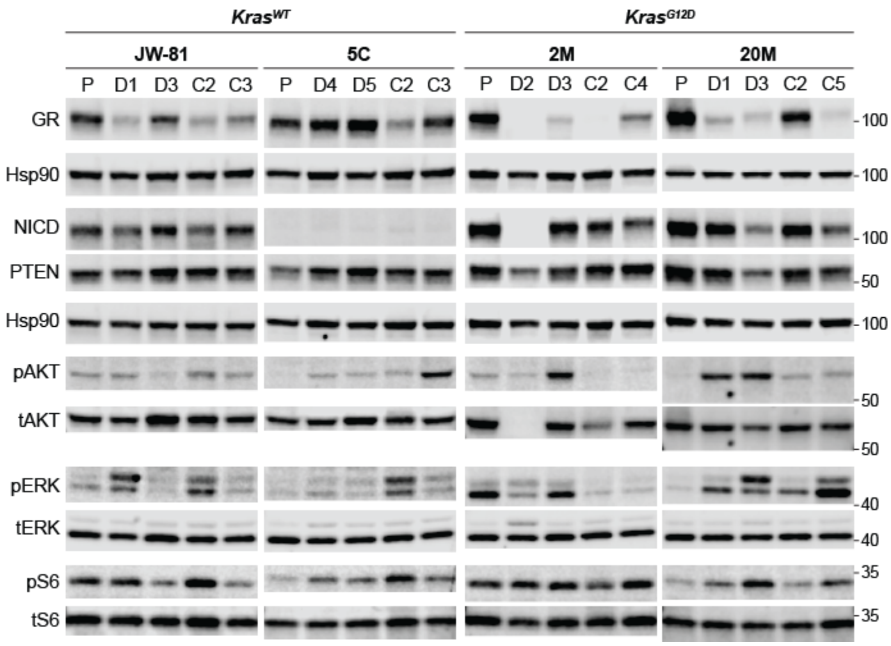

Figure S2. Relapsed murine T-ALL cells lack consistent changes in Ras and Notch1 pathway activation. Western blots were immunoblotted and cropped to assess activation of the Ras and Notch1 pathways through analysis of PTEN, pERK/tERK, pAKT/tAKT, pS6/tS6 and Notch intracellular domain (NICD) protein expression in bone marrow lysates from a panel of parental (P), DEX-treated relapsed (D) and DEX/GDC-0941 combination-treated relapsed (C) primary murine T-ALLs.

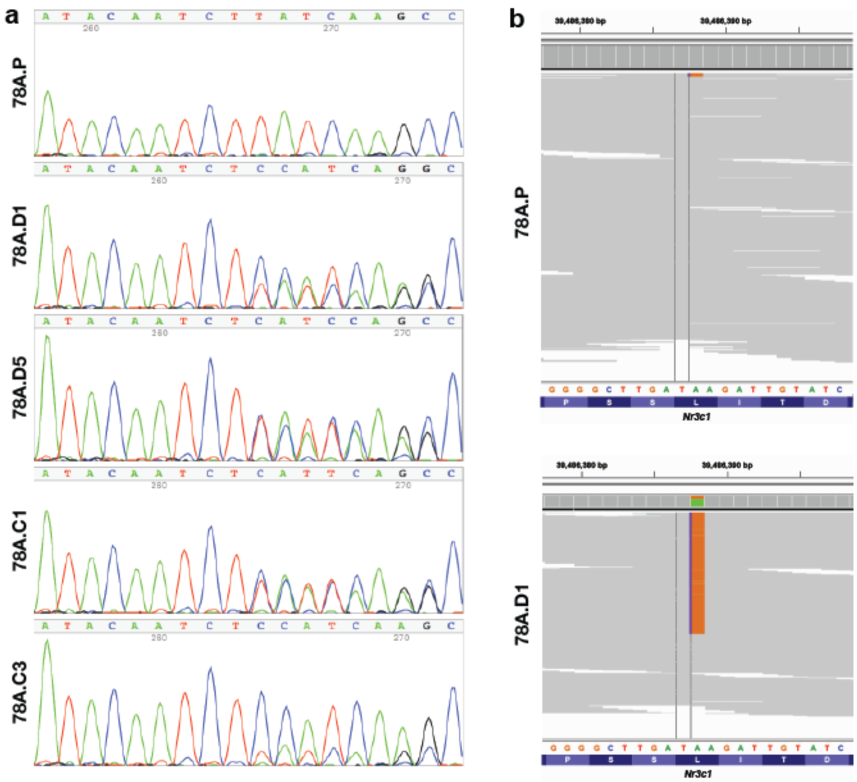

Figure S3. Relapsed T-ALL 78A harbors a pre-existing *Nr3c1* indel. a Sanger sequencing traces of the parental and four DEX-treated relapsed 78A T-ALLs showing the *Nr3c1* indel at varying allele frequencies in relapsed samples analyzed from independent recipient mice. **b** Aligned reads from targeted sequencing data for *Nr3c1* showing the indel allele frequency in the parental sample (78A.P, 1.1%) and in one of the DEX-treated relapsed samples (78A.D1, 62%).

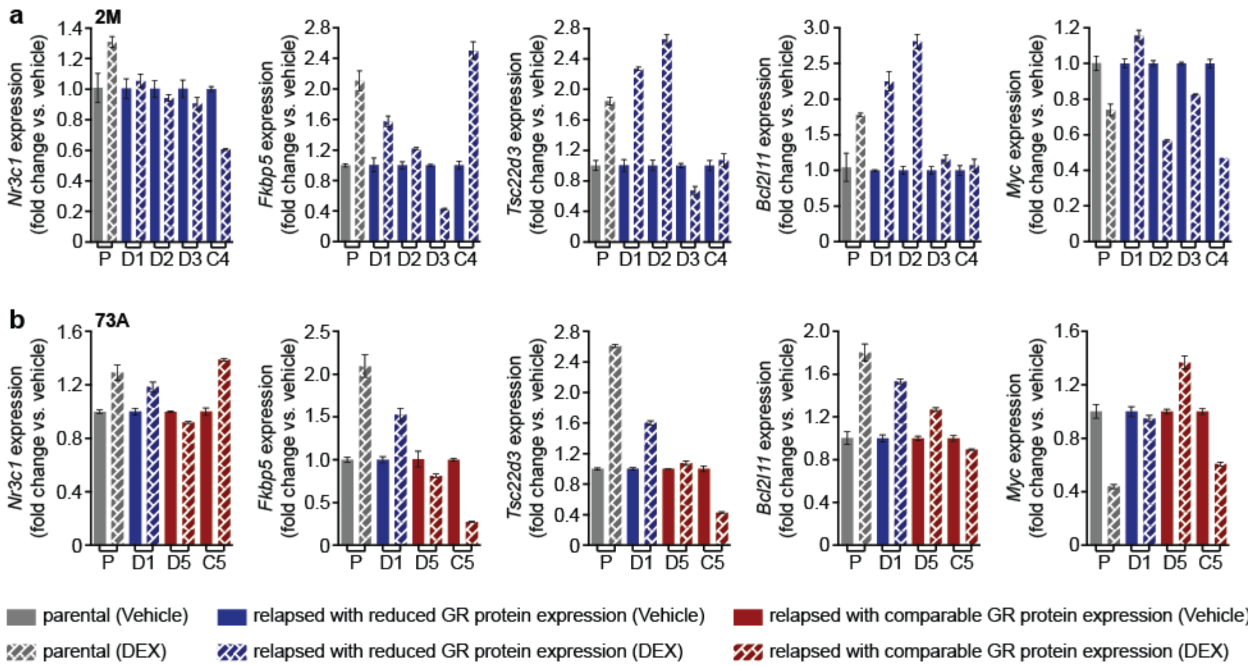

Figure S4. Relapsed T-ALLs show altered transcriptional responses to *in vivo* DEX treatment. Gene expression analysis using TaqMan assays for each indicated GR-responsive gene in parental T-ALLs (P, grey bars), and DEX-treated (D) or DEX/GDC-0941 combination-treated (C) relapsed T-ALLs with reduced (blue bars) or comparable (red bars) GR protein expression as compared to the corresponding parental leukemia after short-term *in vivo* DEX treatment of $Kras^{G12D}$ T-ALLs 2M (**a**) and 73A (**b**). Error bars represent standard error of the mean for technical triplicates.